

## Chapter 4

### Paper III: Stratification-dependent Mixing May Decrease Stability of Atlantic Overturning under Global Warming

# Stratification-dependent Mixing May Decrease Stability of Atlantic Overturning under Global Warming

Ben Marzeion<sup>1</sup>

*Nansen Environmental and Remote Sensing Center, Bergen, Norway*

*Bjerknes Centre for Climate Research, Bergen, Norway*

Anders Levermann

*Potsdam Institute for Climate Impact Research, Potsdam, Germany*

Juliette Mignot

*LOCEAN, Université Pierre et Marie Curie, Paris, France*

submitted to *Geophysical Research Letters*, 2006

**Abstract** We use the Earth System Model of Intermediate Complexity (EMIC) CLIMBER-3 $\alpha$  to investigate the effect of stratification-dependent mixing on the stability of the Atlantic Meridional Overturning Circulation (AMOC) under an idealized CO<sub>2</sub> increase scenario. The vertical diffusivity of the ocean is parameterized as  $\kappa \sim N^{-\alpha}$ , where  $N$  is the local buoyancy frequency. For all parameter values  $0 \leq \alpha \leq 3$ , we find the AMOC to decrease in response to increased CO<sub>2</sub> concentrations. The sensitivity of the AMOC is significantly stronger for  $\alpha \geq \alpha_{\text{cr}} \approx 1.5$ , also after stabilization of the CO<sub>2</sub> concentration. This threshold behavior is explained by a halt of dense water formation in the subpolar gyre, which is caused by a positive feedback between stratification and mixing anomalies.

---

<sup>1</sup>Corresponding author. Ben Marzeion, NERSC, Thormøhlensgate 47, 5006 Bergen, Norway; tel.: +47 55 20 58 83, fax: +47 55 20 58 01, e-mail address: ben.marzeion@nersc.no

## 4.1 Introduction

The Atlantic Meridional Overturning Circulation (AMOC) contributes to the relatively warm northern European climate by transporting  $\sim 1$  PW of heat from the tropics northward (Hall and Bryden 1982; Ganachaud and Wunsch 2000; Trenberth and Caron 2001). The strength of the AMOC is likely to influence global climate, e. g. by modulating the El Niño/Southern Oscillation phenomenon (Timmermann et al. 2005), the position of the Intertropical Convergence Zone (Vellinga and Wood 2002), and by changing the North Atlantic sea level (Levermann et al. 2005). Model results suggest that the influence of increased greenhouse-gas concentrations, by causing decreased heat loss and increased freshwater input in the high latitudes, and thus lowering the density of the surface water in the northern sinking regions, will weaken the future AMOC (Manabe and Stouffer 1994; Rahmstorf and Ganopolski 1999; Gregory et al. 2005; Petoukhov et al. 2005).

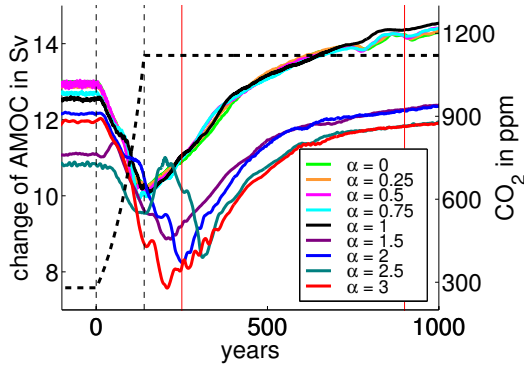


**Figure 4.1:** Timeseries of the anomaly of the maximum AMOC. Black, dashed line:  $\text{CO}_2$  concentration. The vertical lines indicate the beginning and end of the  $\text{CO}_2$  increase (black, dashed) and the time at which the values in figure 4.3 are taken (red).

On long timescales, the AMOC is strongly influenced by the rate of low latitude vertical diffusion (Munk and Wunsch 1998). While some current climate models employ parameterizations for vertical diffusion that take into account bottom roughness and surface conditions (e. g. Gnanadesikan et al.

2006; Jungclaus et al. 2006), most models prescribe diffusivities that are constant in space and/or time in the ocean interior. The fact that diffusion is strongly influenced by stratification (Gargett and Holloway 1984) is thus usually not taken into account. Nilsson and Walin (2001) and Nilsson et al. (2003) argued that a reduction of high latitude surface water density will eventually lead to reduced stratification, which in turn could lead to increased mixing, and an increased overturning. Similar results were found in a box model by Marzeion and Drange (2006). Marzeion et al. (2006) could not reproduce this 'freshwater-boosted' regime in a global coupled climate model, and instead found the stability of the AMOC to be decreased when the sensitivity of mixing on stratification crossed a certain threshold.

Here, we test the sensitivity of the AMOC to increased levels of atmospheric  $\text{CO}_2$  employing stratification-dependent vertical diffusivity.

## 4.2 Model and Experiments

The global coupled climate model CLIMBER-3 $\alpha$  (Montoya et al. 2005) combines a 3-dimensional ocean general circulation model based on the GFDL MOM-3 code with a statistical-dynamical atmosphere model (Petoukhov et al. 2000) and a dynamic and thermodynamic sea-ice model (Fichefet and Maqueda 1997).

For the present study, the vertical diffusivity  $\chi$  is parameterized as

$$\chi = \chi_0 \left( \frac{N}{N_0} \right)^{-\alpha}$$

where  $\chi_0$  is the default diffusivity (set to  $0.2 \cdot 10^{-4} \text{ m}^2\text{s}^{-1}$ ),  $N$  is the local buoyancy frequency, and  $N_0$  is a typical value of the buoyancy frequency at pycnocline depth ( $N_0 = 7.3 \cdot 10^{-3} \text{ s}^{-1}$  in the experiments presented here). The diffusivity is thus increasing with decreasing stratification, with the parameter  $\alpha$  controlling the sensitivity of the mixing to changes in stratification. A more detailed discussion regarding the mixing parameterization can be found in Marzeion et al. (2006).

Since values of  $\alpha$  between 0 and 3 have been identified in measurements in the ocean (Sarmiento et al. 1976; Hoffert and Broecker 1978; Gargett and Holloway 1984; Broecker and Peng 1982; Rehmann and Duda 2000), we choose different values from this range in our experiments. After  $\sim 2000$  yr,

when the model has reached a steady state, the concentration of atmospheric  $\text{CO}_2$  is increased with a rate of  $1\% \text{ yr}^{-1}$  until it reaches the four-fold of the preindustrial value (1120 ppm) after 140 yr. Then the  $\text{CO}_2$  concentration is stabilized (see figure 4.1).

### 4.3 Results

The initial equilibrium state of the AMOC is very similar for all the different values of  $\alpha$ , except for  $\alpha = 1.5$  and  $2.5$ , where the overturning is  $\sim 1$  Sv weaker than in the other cases. The reason for this difference will be discussed below. When the increase of the  $\text{CO}_2$  concentration is started, the overturning weakens. A recovery sets in around the time of stabilization of the  $\text{CO}_2$  concentration, or 100-200 yr later, depending on the value of  $\alpha$  (figure 4.1).

After  $\sim 1000$  yr, when the overturning approaches equilibrium again, two different model states remain, separated by a critical value  $1 \leq \alpha_{\text{cr}} \leq 1.5$ . The difference of the rate of overturning results in differences in the northward heat transport, and temperatures of the north-east Atlantic are found to be  $\sim 2$  K cooler in the supercritical runs ( $\alpha \geq \alpha_{\text{cr}}$ ) compared to the subcritical runs ( $\alpha < \alpha_{\text{cr}}$ ). Note however that the absolute change of temperature remains positive for all values of  $\alpha$  at all times, due to the global warming. In the following, we will describe a feedback mechanism that explains the delay of the recovery, and the difference in the equilibrium states before and after the increase of the  $\text{CO}_2$  concentration.

#### 4.3.1 Two interacting feedbacks

Consider an idealized model of convective mixing: During the summer season, the upper layer receives buoyancy from the atmosphere, and the density difference between the two layers is increased. Diffusion works to reduce the stratification slightly. During the winter season, buoyancy is removed from the upper layer, and convective mixing occurs when the upper layer becomes denser than the deep layers.

Figure 4.2 shows two feedback loops that modify this system when stratification-dependent mixing is employed. There is one direct feedback (dashed arrows) between diffusion and stratification. Its strength is controlled by the value of  $\alpha$ , and it is always at play: An increase in stratification causes a

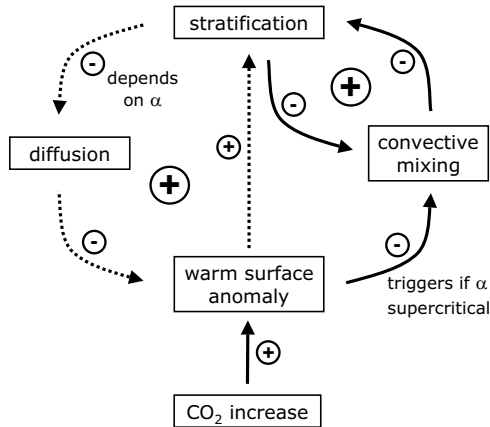


**Figure 4.2:** Illustration of the feedbacks at play in a idealized two-layer model for convective mixing. See text for more details.

reduction in diffusion, which again increases stratification. This feedback loop is relatively weak in equilibrium, but it is enhanced by the warming of the upper layer following increased CO<sub>2</sub> concentrations.

Since it increases the amount of buoyancy stored in the upper layer during summer, it can trigger another strong feedback involving convective mixing (solid arrows in figure 4.2): For supercritical values of  $\alpha$ , the amount of buoyancy is increased to a level where no convective mixing occurs during the winter season. Thus, part of the buoyancy in the upper layer is carried over into the next year, feeding back both on convective mixing, and enhancing the weaker, diffusion-related feedback.

Similar mechanisms were reported by Marzeion et al. (2006) following increased freshwater forcing of the North Atlantic. In the experiments presented in this study, they affect the two areas of dense water formation found in CLIMBER-3 $\alpha$  in different ways, as explained below.

### 4.3.2 Delayed recovery for $\alpha \geq \alpha_{cr}$

During the increase of the CO<sub>2</sub> concentration, the surface water in high northern latitudes get warmer, and fresher because of melting sea ice and

an increased hydrological cycle. The excess surface buoyancy limits the dense water formation, and the overturning gets weaker (figure 4.3a). The recovery of the AMOC after stabilization of the  $\text{CO}_2$  concentration (fig. 4.1) is initiated by the retreat of sea ice, increasing the ocean area exposed directly to the atmosphere in the Nordic Seas (fig. 4.4). This is enough to eventually recover the total buoyancy loss in the area of dense water formation in spite of the global warming (Levermann et al. 2006). Fig. 4.3b shows the resulting recovery of the overturning north of the Greenland-Scotland Ridge.

The timescale of the recovery thus depends on the surface buoyancy flux, and on the amount of excess buoyancy stored in the upper ocean layers that needs to be removed before new dense water formation can set in. The near surface air temperature influences the former directly and indirectly via the sea ice extent. The latter is influenced by  $\alpha$ : following the feedback mechanisms described above, higher values of  $\alpha$  result in a stronger increase of the buoyancy stored in the upper ocean (fig. 4.3b). Assuming that the fluxes between ocean and atmosphere do not change, this means that for higher values of  $\alpha$  more buoyancy needs to be removed from the upper ocean before deep convection can restart, and a stronger reduction in sea ice cover is necessary to restart the dense water formation. This leads to a delay in recovery for  $\alpha \geq \alpha_{\text{cr}}$ .

### 4.3.3 Weaker recovery for $\alpha \geq \alpha_{\text{cr}}$

There are two regions of dense water formation in the model: One area north of the Greenland-Scotland Ridge, and one within the center of the subpolar gyre in the Irminger Sea. During the diminishing phase of the AMOC, dense water formation is weakened in both areas. While in the Nordic Seas dense water formation eventually recovers completely (and even exceeds its initial value, causing the equilibrium AMOC to be stronger at higher  $\text{CO}_2$  concentration), the formation of dense water in the Irminger Sea is weakened for  $\alpha < \alpha_{\text{cr}}$ , and stops completely for  $\alpha \geq \alpha_{\text{cr}}$ .

Figure 4.5 shows the rate of dense water formation in the Irminger Sea as a function of time and  $\alpha$ . These rates were derived by calculating the volume change of waters denser than  $1028 \text{ kg m}^{-3}$  between October and March in the area between  $45^\circ\text{N}$  and  $65^\circ\text{N}$  and between  $10^\circ\text{W}$  and  $40^\circ\text{W}$ . There are two modes of dense water formation in this region: a weak one associated with a weak subpolar gyre, and a strong one associated with a strong subpolar

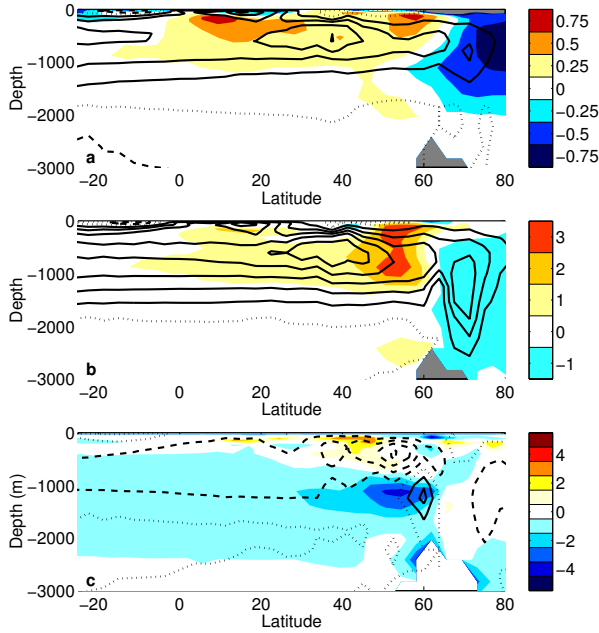


**Figure 4.3:** Upper panel: Shading: Anomaly of the zonally averaged Atlantic salinity for  $\alpha = 2$  in PSU at  $t = 250$  yr. Contours: Atlantic overturning streamfunction for  $\alpha = 2$  at the same time; dotted is zero contour, solid is positive. Contour interval 2 Sv. Middle panel: Shading: Anomaly of the zonally averaged Atlantic temperature change caused by an increase of  $\alpha$ , i. e.  $\Delta T(\alpha = 2) - \Delta T(\alpha = 1)$  in K, taken at  $t = 900$  yr. Contours: Atlantic overturning streamfunction for  $\alpha = 2$  at the same time; dotted is zero contour, solid is positive. Contour interval 2 Sv. Lower panel: Shading: Anomaly of the zonally averaged Atlantic diffusivity change caused by an increase of  $\alpha$ , i. e.  $\Delta \kappa(\alpha = 2) - \Delta \kappa(\alpha = 1)$  in  $10^{-6} \text{m}^2 \text{s}^{-1}$ , taken at  $t = 900$  yr. Contours: Difference of the Atlantic overturning streamfunction  $\Psi$  caused by an increase in  $\alpha$ , i. e.  $\Psi(\alpha = 2) - \Psi(\alpha = 1)$  at the same time; dotted is zero contour, dashed negative, solid positive. Contour interval 1 Sv.

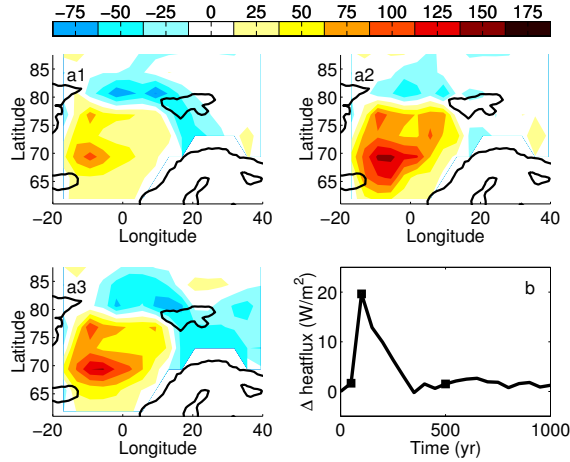


**Figure 4.4:** a: Maps of the heat flux anomaly ( $\text{W/m}^2$ ) into the ocean for  $\alpha=1$ , taken at 50 (a1), 100 (a2), and 500 (a3) years after the start of the  $\text{CO}_2$  increase.  
 b: Timeseries of heat flux anomaly ( $\text{W/m}^2$ ) into the ocean averaged over the area shown in panel a, squares indicate the times of the snapshots shown in panel a.

gyre. All of the unperturbed equilibrium runs, except the runs using  $\alpha = 1.5$  and 2.5, are in the strong subpolar gyre mode before the  $\text{CO}_2$  increase is started. The weaker subpolar gyre is thus the reason for the initially weaker AMOC of those runs as seen in fig. 4.1.

As the  $\text{CO}_2$  concentration increases, the warming of the surface water leads to a weakening of dense water formation. The feedback mechanism discussed in section 3.1 (solid arrows in fig. 4.2) sets in, inducing a larger amount of buoyancy to be accumulated during the summer months for higher values of  $\alpha$ . Since this region is not influenced by changes in sea ice cover, there is no recovery mechanism comparable to the one described in section 3.2, and as the ocean approaches steady state, two regimes of dense water formation remain: for low values of  $\alpha$ , the rates are somewhat reduced, and  $\sim 2$  Sv of dense water are being formed. For  $\alpha \geq \alpha_{\text{cr}}$ , the decrease of diffusivity at the lower edge of the warm anomaly (figure 4.3c) leads to an

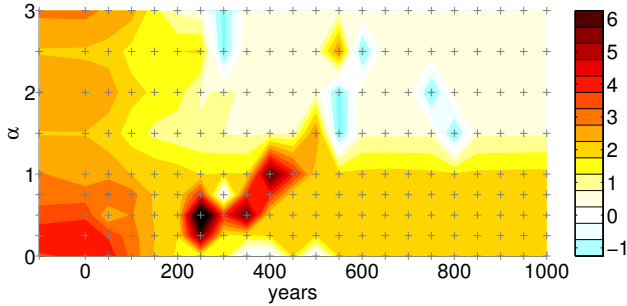


**Figure 4.5:** Rate of dense water ( $\rho \geq 1028 \text{ kg m}^{-3}$ ) production in Sv in the Irminger Sea, as a function of  $\alpha$  and time. Grey crosses indicate positions of data points.

increase of buoyancy in the upper water column that is not removed during winter. As a result, dense water formation is stopped nearly completely. The missing dense water formation in the Irminger Sea then leads to a relative weakening of the AMOC by up to  $\sim 4$  Sv (fig. 4.3c).

## 4.4 Discussion and Conclusions

The model used for the experiments presented here does not account for increased meltwater run-off following the increased  $\text{CO}_2$  levels. It has been argued before that in experiments lacking this feature, the reduced heat fluxes are the dominant effect causing the weakening of the AMOC (Gregory et al. 2005; Levermann et al. 2006). The findings presented here however suggest that additional freshening of the high latitude surface ocean might enhance the strength of the feedback between stratification and diffusion, further destabilizing the AMOC.

The weakening and recovery of the AMOC are only weakly affected by changes of the diffusivity in the pycnocline in low latitudes that are caused by the mixing parameterization: The warm SAT anomaly due to the increased  $\text{CO}_2$  concentration leads to a warming of the surface ocean (fig. 4.3a). As this warm anomaly is penetrating the ocean, it increases stratification at pycnocline depth. This leads to decreased diffusivities, with the magnitude of this effect depending on  $\alpha$  (figure 4.3b). Subsequently, upwelling in low latitudes

is weakened, affecting the strength of the AMOC. However, this effect is of second order: Following the estimates of (Mignot et al. 2006) for the model used in this study, the observed decrease in low latitude vertical diffusivity accounts for  $\sim 0.4$  Sv weakening of the AMOC for  $\alpha = 1$ . This value increases only slightly to  $\sim 0.5$  Sv for  $\alpha = 2$ .

Both the causes for the transient effect leading to the delay of the recovery in the Nordic Seas, and the temperature-related feedback leading to the halt of dense water formation in the Irminger Sea for the supercritical runs are very similar to the mechanism proposed by Marzeion et al. (2006). However, the temperature-related feedback described here has a possible further amplification in the coupling to the atmosphere: While a buoyancy anomaly caused by freshening does not affect the buoyancy exchange with the atmosphere, increased sea surface temperatures lead to a weakening of the temperature contrast found typically in the convective regions, and thus to a further decrease of the buoyancy loss.

CLIMBER-3 $\alpha$  has no atmospheric variability due to the reduced complexity of its atmospheric component, and does not reproduce any convective mixing in the Labrador Sea. Our findings illustrate that the changes of the dense water formation will likely differ strongly between the regions of deep convection. Thus, the experiments presented here can only be a first step in exploring the effect that a more physical parameterization of vertical diffusivity may have on model behavior, and its implications for projections of future climate.

**Acknowledgments** B. M. was supported under the *NOClim 2* project of the *Research Council of Norway*. A. L. and J. M. were supported by the *Gary Comer Foundation*. This is publication nr. XXX of the Bjerknes Centre for Climate Research.

## References

- Broecker, W. S. and T. Peng, 1982: *Tracers in the Sea*. Lamont-Doherty Geological Observatory, Palisades, N. Y.
- Fichefet, T. and M. Maqueda, 1997: Sensitivity of a global sea ice model on the treatment of ice thermodynamics and dynamics. *Journal of Geophysical Research*, **102**, 12609–12646.

- Ganachaud, A. and C. Wunsch, 2000: Improved estimates of global ocean circulation, heat transport and mixing from hydrographic data. *Nature*, **408**, 453–456.
- Gargett, A. E. and G. Holloway, 1984: Dissipation and diffusion by internal wave breaking. *Journal of Marine Research*, **42**, 15–27.
- Gnanadesikan, A., K. W. Dixon, S. M. Griffies, V. Balaji, M. Barreiro, J. A. Beesley, W. F. Cooke, T. L. Delworth, R. Gerdes, M. J. Harrison, I. M. Held, W. J. Hurlin, H. Lee, Z. Liang, G. Nong, R. C. Pacanowski, A. Rosati, B. L. Samuels, M. J. Spelman, R. J. Stouffer, M. Winton, A. T. Wittenberg, and J. P. Dunne, 2006: GFDL's CM2 Global Coupled Climate Models. Part II: The baseline ocean simulation. *Journal of Climate*, **19**, 675–697.
- Gregory, J. M., K. W. Dixon, R. J. Stouffer, A. J. Weaver, E. Driesschaert, M. Eby, T. Fichefet, H. Hasumi, A. Hu, J. H. Jungclaus, I. V. Kamenkovich, A. Levermann, M. Montoya, S. Murakami, S. Nawrath, A. Oka, A. P. Sokolov, and R. B. Thorpe, 2005: A model intercomparison of changes in the atlantic thermohaline circulation in response to increasing atmospheric CO<sub>2</sub> concentrations. *Geophysical Research Letters*, **32**, L12703, doi:10.1029/2005GL023209.
- Hall, M. and H. Bryden, 1982: Direct estimates and mechanisms of ocean heat transport. *Deep-Sea Research*, **29**, 339–359.
- Hoffert, M. I. and W. S. Broecker, 1978: Apparent vertical eddy diffusion rates in the pycnocline of the Norwegian Sea as determined from the vertical distribution of tritium. *Geophysical Research Letters*, **5**, 502–504.
- Jungclaus, J. H., N. Keenlyside, M. Botzet, H. Haak, J. Luo, M. Latif, J. Marotzke, U. Mikolajewicz, and E. Roeckner, 2006: Ocean circulation and tropical variability in the coupled model ECHAM5/MPI-OM. *Journal of Climate*, **19**, 3952–3972.
- Levermann, A., A. Griesel, M. Hofmann, M. Montoya, and S. Rahmstorf, 2005: Dynamic sea level changes following changes in the thermohaline circulation. *Climate Dynamics*, **24**, 347–354.

- Levermann, A., J. Mignot, S. Nawrath, and S. Rahmstorf: 2006, The role of northern sea ice cover for the weakening of the thermohaline circulation under global warming, *Journal of Climate*, in revision.
- Manabe, S. and R. J. Stouffer, 1994: Multiple-century response of a coupled ocean-atmosphere model to an increase of atmospheric carbon dioxide. *Journal of Climate*, 7, 5–23.
- Marzeion, B. and H. Drange, 2006: Diapycnal Mixing in a Conceptual Model of the Atlantic Meridional Overturning Circulation. *Deep-Sea Research Part II*, 53, 226–238.
- Marzeion, B., A. Levermann, and J. Mignot: 2006, The role of stratification-dependent mixing for the stability of the Atlantic overturning in a global climate model, *Journal of Physical Oceanography*, under revision.
- Mignot, J., A. Levermann, and A. Griesel, 2006: A Decomposition of the Atlantic Meridional Overturning Circulation into Physical Components Using Its Sensitivity to Vertical Diffusivity. *Journal of Physical Oceanography*, 36, 636–650.
- Montoya, M., A. Griesel, A. Levermann, J. Mignot, M. Hoffmann, A. Ganopolski, and S. Rahmstorf, 2005: The earth system model of intermediate complexity CLIMBER-3 $\alpha$ . Part I: description and performance for present day conditions. *Climate Dynamics*, 25, 237–263.
- Munk, W. and C. Wunsch, 1998: Abyssal recipes II: energetics of tidal and wind mixing. *Deep-Sea Research Part I*, 45, 1977–2010.
- Nilsson, J., G. Broström, and G. Walin, 2003: The Thermohaline Circulation and Vertical Mixing: Does Weaker Density Stratification Give Stronger Overturning? *Journal of Physical Oceanography*, 33, 2781–2795.
- Nilsson, J. and G. Walin, 2001: Freshwater forcing as a booster of the thermohaline circulation. *Tellus A*, 53, 629–641.
- Petoukhov, V., A. Ganopolski, V. Brovkin, M. Claussen, A. Eliseev, C. Kutzbach, and S. Rahmstorf, 2000: CLIMBER 2: a climate system model of intermediate complexity. Part I: model description and performance for present climate. *Climate Dynamics*, 16, 1–17.

- Petoukhov, V., M. Claussen, A. Berger, M. Crucifix, M. Eby, A. V. Eliseev, T. Fichefet, A. Ganopolski, H. Goosse, I. Kamenkovich, I. I. Mokhov, M. Montoya, L. A. Mysak, A. Sokolov, P. Stone, Z. Wang, and A. J. Weaver, 2005: EMIC Intercomparison Project (EMIP-CO2): Comparative analysis of EMIC simulations of climate, and of equilibrium and transient responses to atmospheric CO<sub>2</sub> doubling. *Climate Dynamics*, **25**, 363–385.
- Rahmstorf, S. and A. Ganopolski, 1999: Long-term global warming scenarios computed with an efficient coupled climate model. *Climatic Change*, **43**, 353–367.
- Rehmann, C. R. and T. F. Duda, 2000: Diapycnal Diffusivity Inferred from Scalar Microstructure Measurements near the New England Shelf/Slope Front. *Journal of Physical Oceanography*, **30**, 1354–1371.
- Sarmiento, J. L., H. W. Feely, W. S. Moore, A. E. Bainbridge, and W. S. Broecker, 1976: The Relationship Between Vertical Eddy Diffusion and Buoyancy Gradient in the Deep Sea. *Earth and Planetary Science Letters*, **32**, 357–370.
- Timmermann, A., S. An, U. Krebs, and H. Goosse, 2005: ENSO suppression due to weakening of the north atlantic thermohaline circulation. *Journal of Climate*, **18**, 2842–2859.
- Trenberth, K. E. and J. M. Caron, 2001: Estimates of meridional atmosphere and ocean heat transports. *Journal of Climate*, **14**, 3433–3443.
- Vellinga, M. and R. A. Wood, 2002: Global climatic impacts of a collapse of the atlantic thermohaline circulation. *Climatic Change*, **54**, 251–267.